Title

A Novel Galectin-1 Inhibitor Discovered through One-Bead Two-Compound Library Potentiates the Antitumor Effects of Paclitaxel *in vivo*.

Journal

Molecular cancer therapeutics, 16(7)

ISSN

1535-7163

Authors

Shih, Tsung-Chieh
Liu, Ruiwu
Fung, Gabriel
et al.

Publication Date

2017-07-01

DOI

10.1158/1535-7163.mct-16-0690

Peer reviewed

Small Molecule Therapeutics

Molecular Cancer Therapeutics

A Novel Galectin-1 Inhibitor Discovered through One-Bead Two-Compound Library Potentiates the Antitumor Effects of Paclitaxel *in vivo*

Tsung-Chieh Shih[1], Ruiwu Liu[1], Gabriel Fung[1], Gaurav Bhardwaj[2], Paramita M. Ghosh[1,3,4], and Kit S. Lam[1]

Abstract

Through the one-bead two-compound (OB2C) ultra–high-throughput screening method, we discovered a new small-molecule compound LLS2 that can kill a variety of cancer cells. Pull-down assay and LC/MS-MS indicated that galectin-1 is the target protein of LLS2. Galectin-1 is known to be involved in the regulation of proliferation, apoptosis, cell cycle, and angiogenesis. Binding of LLS2 to galectin-1 decreased membrane-associated H-Ras and K-Ras and contributed to the suppression of pErk pathway. Importantly, combination of LLS2 with paclitaxel (a very important clinical chemotherapeutic agent) was found to exhibit synergistic activity against several human cancer cell lines (ovarian cancer, pancreatic cancer, and breast cancer cells) *in vitro*. Furthermore, *in vivo* therapeutic study indicated that combination treatment with paclitaxel and LLS2 significantly inhibits the growth of ovarian cancer xenografts in athymic mice. Our results presented here indicate that the OB2C combinatorial technology is a highly efficient drug screening platform, and LLS2 discovered through this method can be further optimized for anticancer drug development. *Mol Cancer Ther; 16(7); 1212–23. ©2017 AACR.*

Introduction

Plasma membrane proteins exhibit various functions involving ion transport, cell adhesion, and sensory stimuli transduction (1). Some of them play a pivotal role in human diseases such as cancer [death receptor, G protein–coupled receptor, EGFR, TNF receptor, and Toll-like receptors (TLR)] (2–5). In particular, death receptor present on the plasma membrane of cancer cells can be activated by chemical compounds to induce cell apoptosis. Therefore, membrane proteins are attractive therapeutic targets for anticancer drug development (6). Among the pharmaceutically active heterocyclic compounds, the benzimidazole ring is an important pharmacophore (7). It might be fruitful to develop methods to synthesize large number of benzimidazole derivatives and screen them efficiently against cell surface receptors for biologic properties, such as anticancer activities.

The one-bead one-compound (OBOC) combinatorial library method was developed as an ultra–high-throughput method for synthesis and screening of chemical compounds, including peptides, peptidomimetics, small molecules, and macrocyclic natural products like molecules (8), for specific biological properties. Using "split-mix" synthesis method, millions of compounds can be rapidly synthesized on-bead. Functional compounds can then be screened by directly mixing the compound beads with the target protein. Beads interacting with the target are isolated and chemically decoded by Edman degradation or mass spectrometry (9, 10). The OBOC method has widespread applications in the search for new bioactive compounds. For example, Peng and colleagues used this approach to identify a novel high-affinity peptidomimetic against α4β1 integrin (11). One-bead two-compound (OB2C) method was first introduced by Meldal and colleagues. They constructed fluorescence-quenched substrate libraries for investigation of protease activity and successfully identified protease inhibitors (12). We later applied the OB2C concept to facilitate the discovery of proapoptotic peptides that target cell surface (13). In such OB2C libraries, each bead displays two compounds: a hexapeptide library compound (OBOC format) and a fixed well-defined cell adhesion ligand (second compound). When live cells are incubated with the OB2C bead library, each bead will be covered with a layer of cells by the action of the cell capturing or adhesion ligand, thus exposing their cell membrane proteins to the OB2C library compounds. Screening was performed by propidium iodide (PI) staining that can be used to identify dead cells. With this approach, two peptidic death ligands against T-cell leukemia cells (Molt-4) were identified (13).

Galectin-1, a 14-kDa lectin, is one of the galectin family members with an affinity for β-galactosides. High expression of galectin-1 has been found in many human cancers, including ovarian cancer (14), prostate cancer (15), lung cancer (16), breast cancer (17), kidney cancer (18), and pancreatic cancer (19). High expression of galectin-1 is directly implicated in the process of tumorigenesis (20, 21). Galectin-1 is involved in cancer progression and also associated with a poor prognosis in prostate, lung, and ovarian cancers. Galectin-1 can localize to both intracellular and extracellular space. Intracellular galectin-1 binds to oncogenic H-Ras and activates pERK signaling pathway, resulting in cell

[1]Department of Biochemistry and Molecular Medicine, University of California Davis, Sacramento, California. [2]Department of Biochemistry, University of Washington, Seattle, Washington. [3]Department of Urology, University of California Davis, Sacramento, California. [4]VA Northern California Health Care System, Sacramento, California.

Note: Supplementary data for this article are available at Molecular Cancer Therapeutics Online (http://mct.aacrjournals.org/).

Corresponding Authors: Kit S. Lam and Ruiwu Liu, University of California at Davis, 2700 Stockton Blvd, Sacramento, CA 95817. Phone: 916-734-0910; Fax: 916-734-4418; E-mail: kslam@ucdavis.edu and rwliu@ucdavis.edu

doi: 10.1158/1535-7163.MCT-16-0690

transformation (22). Galectin-1 secreted by tumor cells exerts tumor immunosuppression through the induction of apoptosis of activated T cells (23, 24) and stimulates tumor angiogenesis via the interaction of VEGFR2 (25). Recent articles reported that galectin-1 exhibits an oncogenic activity through the activation of H-Ras/Raf/ERK pathway, p21 and Bcl-2 in ovarian cancer (14), HIF/mTOR pathway in clear cell renal cell carcinoma (18), and Hedgehog pathway in pancreatic cancer (19)

In this study, we adapted the powerful OB2C combinatorial library method for the discovery of synthetic death ligands against ovarian cancer in an ultra–high-throughput fashion. In these OB2C benzimidazole libraries, each bead displays on its surface an ovarian cancer cell–capturing molecule LXY30 (an α3β1 integrin binding ligand; ref. 26) and a benzimidazole library compound prepared by split and mix synthesis. When the bead library is incubated with SKOV-3 ovarian cancer cells that express high level of α3β1 integrin, each and every compound-bead is coated with cells. Cells that undergo apoptosis can be readily detected by immunocytochemistry (ICC) using anti-cleaved caspase-3 antibody, and compound beads coated with stained cells are considered candidate death ligands. Two death ligands against SKOV-3 cells have been identified from an OB2C benzimidazole-based small-molecule library (74,088 permutations), and their proapoptotic effects have been confirmed. One of these ligands, LLS2, was active against SKOV-3 cells at low micromolar IC_{50}. Pull-down assay followed by LC/MS-MS indicated that galectin-1 is the target protein of LLS2. Molecular modeling studies suggested that LLS2 binds to the interface between the dimeric galectin-1 subunit, and is within 6 Å from the β-galactoside binding pocket. Binding of LLS2 to galectin-1 decreases membrane-associated Ras and contributes to the suppression of pERK pathway. *In vivo* study showed that LLS2 suppressed tumor growth in SKOV3 xenograft mice. Moreover, LLS2 was found to potentiate the antitumor activity of paclitaxel, both *in vitro* and *in vivo*.

Materials and Methods

Construction of OB2C library

In OB2C library, a biotin molecule is codisplayed with library compound or testing molecule on the surface of the bead. Biotin is the site to introduce a cell-capturing ligand after biotinylated ligand–streptavidin (3:1) complex is incubated with the library beads. Here, we used biotinylated LXY30, a high-affinity ligand against α3β1 integrin, which is overexpressed in many epithelial cancers, including SKOV3 ovarian cancer cells. The detailed procedure is described in Supplementary Material.

Synthesis of death ligands on beads and in soluble form

LLS1 and LLS2 were resynthesized on TentaGel resin in an OB2C format for validation of proapoptotic activity. For detail of synthesis, please refer to Supplementary Material. Soluble LLS2 and biotinylated LLS2 (LLS2-biotin) were synthesized on Rink amide resin using similar chemistry described in library synthesis. LLS2-biotin was designed to have biotin attached to the side chain of Lys, and two hydrophilic linkers between LLS2 and Lys(biotin). Detailed synthetic procedures of LLS2 and LLS2-biotin are described in Supplementary Material. The final products were cleaved off the beads with trifluoroacetic acid (TFA) cocktail, precipitated with cold ether and purified by reverse-phase high-performance liquid chromatography (HPLC). Although the starting scaffold used for synthesis of LLS2 and LLS2-biotin is racemic, by introducing another stereocenter from (*S*)-L-(3,4-diCl)phenylalanine, the final products formed two diastereoisomers that were successfully separated by HPLC with optimized conditions. LLS2 was found as the major diastereoisomer with (R, S) configuration at approximate ratio of 9:1 over its (S, S) isomer, which was determined by HPLC peak integration.

Cell lines

The cell lines, including human ovarian cancer cell line SKOV3, the lung cancer cell line A549, the prostate cancer cell line PC3, the pancreatic carcinoma cell line XPA3, the breast cancer cell line MCF7, and normal kidney cell line (MDCK), were obtained from the ATCC. Galectin-1 was examined by Western blotting after transfection with siGal-1 and pcDNA/Gal-1. Mycoplasma testing was routinely performed every month; no additional authentication was done by the authors.

ICC assay on beads

First, we reacted neutravidin (5 nmol) with LXY30-biotin in 1:2 molar ratio for 20 minutes. After gluing the OB2C beads onto the 12-well culture plate with 80% dimethylformamide, mixture of neutravidin and LXY30-biotin was added onto the beads-glued wells. After 20 minutes of incubation, SKOV3 cells (5×10^5) were then seeded onto the well and incubated at 37°C for 20 minutes. The unbound cells were removed by gentle washing with PBS. Cell-bound beads were incubated at 37°C for another 24 hours, followed by fixation in 4% paraformaldehyde for 20 minutes. For ICC assay on beads, nonspecific protein binding was blocked by adding 5% BSA, and cell membrane was permeabilized with 0.5% Triton X-100. We used rabbit anti-human cleaved caspase-3 (Cell Signaling Technology) as the primary antibody. Beads were incubated with primary antibody (1:100 in PBS) overnight at 4°C. After washing with PBS, beads were then incubated with the secondary antibody, an HRP-conjugated goat anti-rabbit IgG, for 1 hour at room temperature. HRP activity was finally detected using diaminobenzidine tetrahydrochloride as a substrate for 3 minutes according to the manufacturer's instructions (BioGenex).

Decoding of positive beads

Positive beads were isolated, followed by treatment with 6 mol/L guanidine HCl (pH 1.0), to remove the bound cells or any proteins or biomolecules produced by the cells, and washed with water thoroughly prior to chemical decoding using standard automatic Edman microsequencing (ABI Procise 494).

Cell survival assay

For immobilized LLS2, streptavidin-coated plates were loaded with LLS2-biotin. SKOV3 cells (3×10^3) were seeded in these LLS2-coated plates. After 72 hours, cell survival assay was assessed using CellTiter-Glo Luminescent Cell Viability Assay Kit (Promega). For solution phase cytotoxic assay, 3×10^3 SKOV3 cells were seeded into 96-well plates. After 24 hours, medium was removed and the cells were treated with the indicated concentrations of LLS2, and cell viability was determined after 72 hours. Briefly, the CellTiter-Glo reagent was diluted by CellTiter-Glo Buffer. Diluted reagent (100 μL) was added to plate with wells containing cells and culture medium. The plates were incubated at

room temperature for 10 minutes, and the luminescence was quantified by plate reader (PerkinElmer).

PI staining on beads

After 48 hours, bead-bound cells were stained with 1 μg/mL PI for 10 minutes. After one wash with PBS, cells were photographed using a fluorescence microscope (Olympus IX81).

Analyses of combination index

The combination index (CI), computed with the multiple drug effect equation of Chou–Talalay, has been widely used to quantify drug synergism. In our study, the CI values were determined for the drug combination in cell proliferation assays using CalcuSyn software. CI <0.9 indicates synergism, CI = 0.9–1.10 indicates additive interaction, and CI >1.10 indicates antagonism (27).

Pull-down assay

SKOV3 cells (2×10^6) were cultured for membrane protein extraction using a commercial kit (ProteoExtract Native Membrane Protein Extraction Kit, Millipore). Streptavidin agarose gel slurry (50 μL; Pierce) was mixed with 50 μg biotinylated LLS2-biotin in the spin column. The mixture was incubated at 4°C for 2 hours followed by centrifugation at 1,250 × *g* for 1 minute at room temperature. After washing with TBS, agarose gel was incubated with 20 μg membrane protein overnight at 4°C. Agarose gel beads were washed three times with TBS, and then, protein was eluted with 250 μL elution buffer (150 mmol/L glycine-HCl, pH 1.5–2.5). The eluent was then neutralized by adding 10 μL neutralization buffer (Tris, pH 8.0). The eluted protein was digested by incubating overnight at 37°C with trypsin (Promega; at 5 ng/mL) and subjected to mass spectrometry (MS) analysis (28).

Protein identification by MS/MS

The eluted protein was then digested by incubating overnight at 37°C with trypsin at 5 ng/mL (Promega) in 50 mmol/L NH_4HCO_3 buffer, pH 7.8. Tryptic peptides were extracted from the gel pieces in 1 volume of 0.1% trifluoroacetic acid, while vortexing for 5 minutes, followed by sonication for 5 minutes. Crude digest mixtures were concentrated and desalted using mC18 ZipTips (Millipore), followed by eluting in 1.5 mL of matrix (5 mg of CHCA/mL in 50% ACN/0.1% TFA) for matrix-assisted laser desorption/ionization—time-of-flight (MALDI-TOF) MS and MS/MS analyses. Both MS and MS/MS spectra were searched against the NCBI database, using MASCOT software from matrix science (www.matrixscience.com), to identify the proteins. The MALDI-TOF MS resolution for the peptides was around 20,000, and the mass accuracy was 0.01 to 0.02 Da. The MS/MS resolution was around 6,000.

Plasmids and siRNA transfections

SKOV3 and HT29 cells (5×10^3) were seeded on the 96-well plate and transfected with siRNA against galectin-1 (200 nmol/L; Ambion) and pcDNA/gal-1 (100 ng; GenScript), respectively. MDCK cells (1×10^5) were seeded on the 6-well plate and transfected with H-Ras(G12V), K-Ras(G12V), and N-Ras (Q61K) plasmids (2 μg; Addgene). Transfection was performed using Lipofectamine 3000 transfection reagent (Life Technologies) according to the manufacturer's instructions. MDCK transfected cells were selected using 2 μg/mL puromycin after additional 7 days.

Ras activation assay

Stable K-Ras (G12V) and N-Ras (Q61K) transfected cells were serum starved overnight. The cells were stimulated with 100 ng/mL EGF for 20 minutes, followed by treatment with 25 μmol/L of LLS2 for 2 hours. Cells were lysed and Raf-1 Ras-binding domain-agarose beads (Millipore) were added to cell lysates for 30 minutes at 4°C followed by centrifugation at 14,000 × *g* for 10 seconds at 4°C. After washing, the agarose-bound Ras was incubated in 2× Laemmli reducing sample buffer (126 mmol/L Tris/HCl, 20% glycerol, 4% SDS, 0.02% bromophenol blue) followed by electrophoresis and Western blotting with an anti-Ras antibody (Millipore).

Immunoblotting analysis

SKOV3 and A549 cells were serum starved overnight, and the cells were then treated with 100 ng/mL EGF for 20 minutes following treatment with LLS2 (25 μmol/L) for 2 hours. Cells were lysed in a RIPA lysis buffer (50 mmol/L Tris-HCl pH 7.5, 0.5% sodium deoxycholate, 1% NP-40, 0.1% SDS, 150 mmol/L NaCl, 2 mmol/L EDTA, 50 mmol/L NaF, 1 mmol/L DTT, 2 mg/mL aprotinin, and 2 mg/mL leupeptin) and incubated on ice for 20 minutes. After centrifugation at 12,000 × *g* for 20 minutes at 4°C, total cell lysates were collected. Twenty micrograms of each lysate was boiled in 2× Laemmli SDS-PAGE sample buffer (126 mmol/L Tris/HCl, 20% glycerol, 4% SDS, 0.02% bromophenol blue) at 95°C for 10 minutes, followed by separation on 12% SDS-PAGE gels and transferred onto PVDF membrane (Bio-Rad). After blocking with 10% nonfat dried milk for 1 hour, the membrane was incubated with the specific primary antibodies against phospho-MEK, MEK, phosphor-Erk, Erk, β-actin (Cell Signaling Technology) at 4°C overnight followed by incubation with corresponding secondary antibodies at 37°C for 1 hour. After addition of ECL substrate (Amersham), chemiluminescence signal was detected by CCD camera (Bio-Rad).

ICC

For light microscopy, cells were fixed in 4% paraformaldehyde. Nonspecific protein binding was blocked by adding 5% BSA. We used rabbit antihuman galectin-1 (Abcam) or LLS2-biotin as primary antibody or primary ligand, respectively. Cells were incubated with primary antibody (1:200 in PBS) overnight at 4°C. After washing with PBS, cells were then incubated with the secondary antibody, a rhodamine-conjugated goat anti-rabbit IgG (The Jackson Laboratory) or FITC-conjugated streptavidin (Sigma) in the case of primary ligand, for 1 hour at room temperature. Finally, the cells' nuclear DNA was stained with DAPI (Invitrogen). After washing, the cells were mounted and photographed using a confocal microscope (Zeiss).

IHC

Tissue sections were dewaxed using xylene twice and rehydrated with 100% ethanol for 5 minutes, 95% and 80% ethanol for 5 minutes each, and then rinsed in PBS. Antigen retrieval was performed in 10 mmol/L, pH 6.0 sodium citrate buffer at 95°C to 100°C for 20 minutes. After cooling down to room temperature, tissue sections were rinsed with PBS once followed by blocking endogenous peroxidase with 1% H_2O_2 and blocking nonspecific

binding site with Power Block (BioGenex) for 5 minutes at room temperature each. The tissue sections were then incubated with the specific antibody against cleaved caspase-3 and Ki-67 (Cell Signaling Technology) overnight and rinsed extensively three times with PBS. Nuclei were counterstained with hematoxylin. For secondary antibody labeling, the same protocol as in ICC was used in IHC.

In vivo xenograft tumor assays

Paclitaxel and LLS2 were prepared in 50% absolute alcohol and 50% Cremophor to make a 6 and 30 mg/mL solution, respectively. Prior to administration, it was diluted with saline to produce 1 and 5 mg/mL solution, respectively. Female congenital athymic BALB/c nude (nu/nu) mice were purchased from The Jackson Laboratory. SKOV3 cells (2.5×10^6) were subcutaneously injected to the right side of the mouse dorsal flank. The tumors were allowed to grow to about 100 mm^3. Then, mice were randomly divided into control and treatment groups, and each group contained 5 mice. Mice were given a daily intravenous administration for 5 successive days. Tumor size and body weight were measured every 3 days. In our previous study, the 10 mg/kg paclitaxel did not significantly inhibit tumor growth (29). Eighteen days after implantation, mice were sacrificed and tumor were excised, fixed in 10% formaldehyde, embedded in paraffin, and finally sectioned for histopathology examination.

Statistical analysis

All the *in vitro* experimental studies were performed in triplicate in two different experiments. The χ^2 test or the Student t test was used for comparison between variables. All results were expressed as the mean ± SD, and a value of $P < 0.05$ was considered statistically significant.

Results

Construction of OB2C library

In this library, each bead displays on its surface a biotin and a benzimidazole library compound. Desirable cell-capturing molecule such as LXY30 (an α3β1 integrin binding ligand) can be conveniently displayed on the bead surface, by premixing LXY30-biotin with streptavidin at 3:1 ratio, and then added to the bead library. The coding tag is a tripeptide that resides inside the bead, such that it will not interfere with the screening. Figure 1 shows the synthetic scheme. The benzimidazole library has three diversities, constructed from 42 primary amines (R_1NH_2), 42 aldehydes (R_2CHO), and 42 amino acids (X_3, including L- and D-amino acids, natural and unnatural amino acids). The total permutation of the OB2C-S3 library is calculated to be 74,088 ($42 \times 42 \times 42$).

High-throughput screening using ICC assay on beads

Caspase-3, a pivotal executioner of apoptosis, is activated by cleavage into p20 and p12 fragments and proteolytically cleaves several intracellular substrates (30). We believe an efficient colorimetric assay to detect cleaved caspase-3 in fixed cells will be an excellent approach to screen OB2C libraries for proapoptotic ligands. We used anti-cleaved caspase-3 antibody to perform ICC staining of cells bound on library beads. A positive cell-bound bead is shown in Fig. 2A and B. For the discovery of death ligands against SKOV3 cells, a total of about 80,000 beads from OB2C-S3 library were screened; two positive beads were detected. These two positive beads were physically isolated by hand-held micropipette and their chemical identity determined by chemical decoding of the peptide tag with automatic Edman microsequencing. To validate the proapoptotic activity of these lead compounds, we first synthesized the death ligands on beads and then stained the

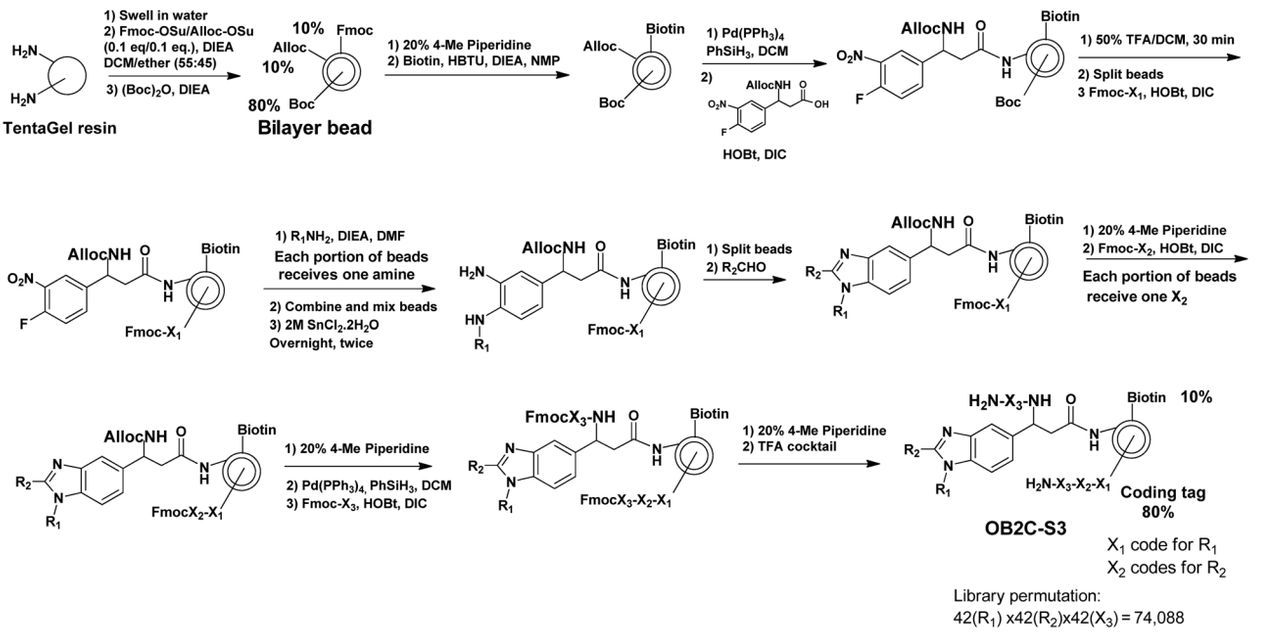

Figure 1.

Synthetic scheme of library OB2C. The library was synthesized on topologically segregated bilayer TentaGel beads using split-mix synthesis method. The library has three diversities from 42 primary amines (R_1NH_2), 42 aldehydes (R_2CHO), and 42 amino acids (X_3) containing both L- and D-amino acids, and natural and unnatural amino acids, respectively.

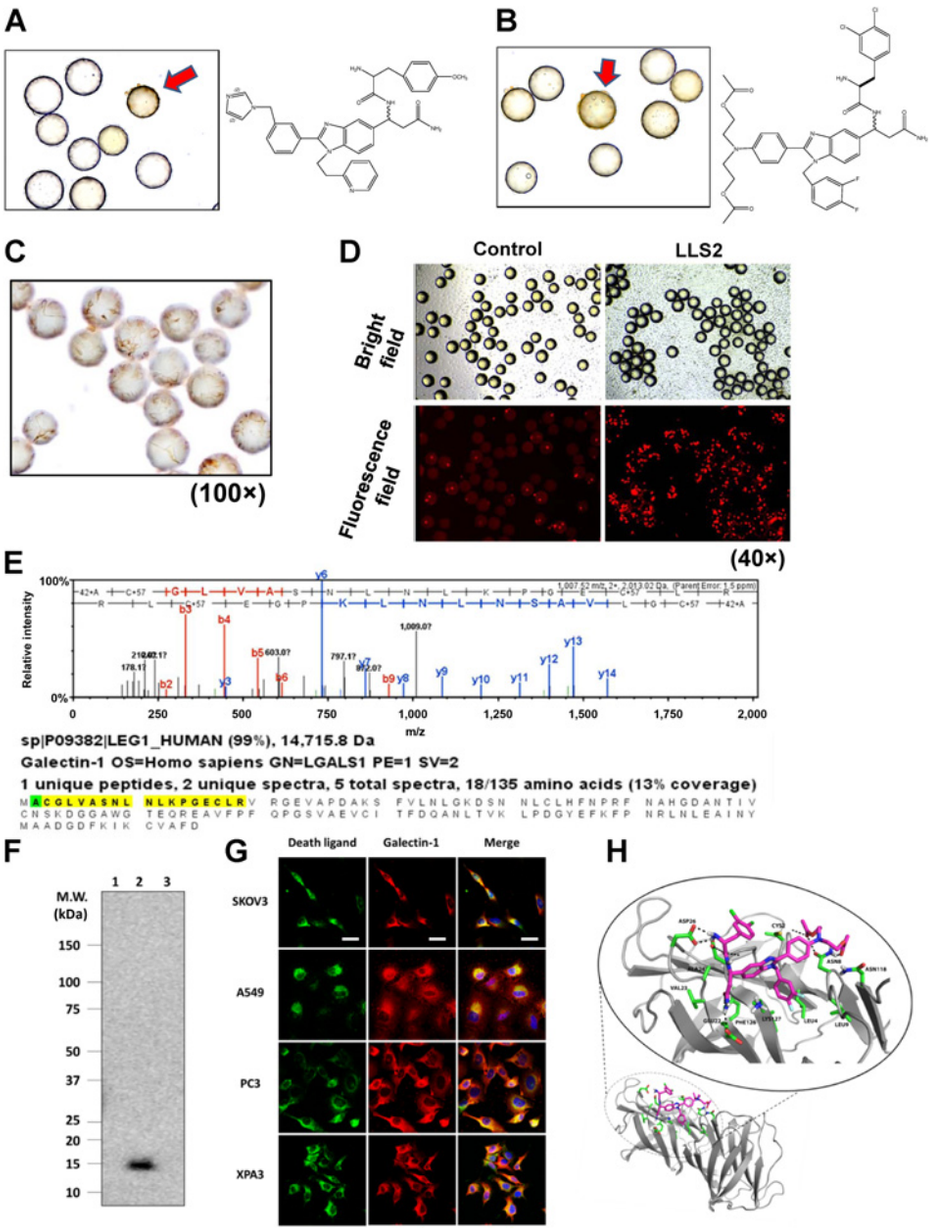

Figure 2.
Screening OB2C small-molecule library for death ligands. Cleaved caspase-3–positive beads (red arrow) in OB2C beads library. Positive beads were picked up for chemical decoding with automatic Edman microsequencing. **A,** LLS1. **B,** LLS2. Resynthesize death ligand LLS2 on beads for validation of death effect. **C,** Cleaved caspase-3 staining (100×) **D,** PI staining for dead cells (40×). Galectin-1 is a target protein of LLS2. **E,** Eluted protein from pull-down assay was identified as galectin-1 by LC MS/MS. **F,** Immunoblot analysis with anti-galectin-1 Ab to validate the LC/MS-MS result. 1: blank bead, 2: LLS2-beads, 3: an irrelevant small-molecule bead control. **G,** Immunostaining result reveals that LLS2 colocalizes with galectin-1. SKOV3, A549, PC3, and XPA3 cells were stained by biotinylated LLS2 (green), galectin-1 antibody (red), and nuclei were stained with DAPI (blue). **H,** Computer modeling shows that LLS2 binds the interface of the galectin-1 dimer. Residues that are within 3.5 Å from LLS2 are shown. Scale bars, 50 μm.

bound cell for caspase-3 cleavage products. Our ICC data indicated that LLS2 indeed has the ability to induce caspase-3, which is consistent with the screening results (Fig. 2C). In addition to confirming early apoptosis by caspase-3 staining on beads, we also validated cell death by PI, which stains late apoptotic cells with leaky cell membrane (31). After 48 hours of binding with beads displaying LLS2, SKOV3 cells were stained with PI. Many PI-positive cells were detected (Fig. 2D).

Galectin-1 is a target protein of LLS2

To clarify the molecular mechanism of LLS2 causing cell death, we used pull-down assay to determine the target protein of LLS2. SKOV3 cell membrane proteins bound to biotinylated LLS2 were first retained by streptavidin resin. Eluted proteins analyzed by LC/MS-MS revealed galectin-1 as the putative target protein (Fig. 2E). The identity of galectin-1 as the target protein of LLS2 was further supported by immunoblot analysis of proteins (Fig. 2F) eluted from (i) blank streptavidin beads; (ii) LLS2-biotin/streptavidin beads; and (iii) biotinylated unrelated small-molecule/streptavidin beads, using anti-galectin-1 antibody as the Western blot probe. As shown in Fig. 2F, a 14-kDa protein corresponding to galectin-1 was identified in lane 2 only, in which LLS2 was used as the affinity ligand, indicating that the target protein of LLS2 was indeed galectin-1. We then separately stained fixed and permeated SKOV3 cells with (i) LLS2-biotin followed by streptavidin-fluorophore, and (ii) anti-galectin-1 antibody and demonstrated that fluorescent signals elicited by LLS2 and galectin-1 colocalized (Fig. 2G).

The putative binding site of LLS2 to dimeric galectin-1, predicted by computer modeling, is shown in Fig. 2H. We performed

multiple computational docking simulations to understand the binding of LLS compounds to galectin-1 monomer and dimer structures. Blind docking studies were first performed to rapidly scan the protein surface to identify putative binding surfaces. These initial studies were followed by the more accurate and fine-grained docking simulations across the previously identified binding interfaces. These docking studies of LLS2 with galectin-1 dimer suggest stable binding interactions that span both components of the homodimeric complex (Fig. 2H). LLS2 shows good shape complementarity with the dimer-binding pocket. The "R_2" group of LLS2 forms hydrogen bond networks with the galectin-1 dimer, while the aromatic groups of LLS2 pack nicely against the hydrophobic core of the binding pocket.

LLS2 affects H-Ras(G12V) and K-Ras(G12V) localization

To elucidate the molecular mechanisms of LLS2 on tumor regression, the expression level and activity of signaling molecules associated with galectin-1 were analyzed. Galectin-1 located in cytoplasmic membrane (32) is known to cooperate with H-Ras in cell signaling and transformation (Fig. 3A). As activated H-Ras (G12V) at the plasma membrane is essential for induction of oncogenic signaling pathway and its association with plasma membrane is stabilized by galectin-1 (22), we investigated whether membrane-associated H-Ras(G12V) can be affected by LLS2. Real-time confocal images of EGF-treated cells revealed that GFP-H-Ras(G12V) fusion resided on the plasma membrane migrated to intracellular compartments after treatment with LLS2 (25 μmol/L) for 30 minutes (Fig. 3B). This is further supported by Western blot analysis of plasma membrane, which showed that membrane-associated H-Ras level of MDCK cells was greatly diminished after treatment with LLS2 (Fig. 3C). LLS2 treatment was also found to (i) induce miscolocalization of the EGF-stimulated K-Ras(G12V) fusion, but not the EGF-stimulated N-Ras (Q61K) fusion (Fig. 3D), and (ii) decrease the EGF-stimulated levels of K-Ras-GTP (Fig. 3D and E). An important downstream effect of Ras pathway is the activation of pErk, which is required for cell survival, transformation, proliferation, and migration (33). We next examined the effect of LLS2 on MAPK/ERK pathway. Expression level of phospho-MEK and phospho-Erk was found to be downregulated in SKOV3 and A549 cells after treatment with LLS2 for 24 hours (Fig. 3F). Together, the data support our notion that LLS2 induces cell death through suppression of the Ras–Erk pathway.

***In vitro* anticancer activity of LLS2**

Immunoblots show that high expression level of galectin-1 was found in colon cancer cell line HT29, prostate cancer cell line PC3, ovarian cancer cell line SKOV3, pancreatic cancer cell line XPA3, breast cancer cell line MCF7, and lung cancer cell line A549PC3 (Fig. 4A). We then tested the killing effect of the LLS2 compound in solution. Notably, we found that LLS2 killed SKOV3 cells with an IC_{50} value of 15.7 μmol/L (Fig. 4B). In addition, LLS2 can kill HT29, PC3, XPA3, MCF7, and A549 with an IC_{50} value of 24.5, 28.2, 20.9, 23.2, and 34.3 μmol/L, respectively. To further evaluate the specificity of galectin-1 as the target for LLS2 effect, we used siRNA to downregulate galectin-1 in SKOV3 cells and pcDNA/galectin-1 to overexpress galectin-1 in HT29 cells (Fig. 4C). We found that SKOV3 cells transfected with negative control siRNA were more sensitive to LLS2 than those transfected with galectin-1 siRNA (Fig. 4D). Conversely, ectopic expression of galectin-1 increased sensitivity of HT29 cells to LLS2 (Fig. 4D). Although we cannot rule out the possibility of other therapeutic targets for LLS2, the result support our notion that the major mechanisms of action of "death" function of LLS2 are through the inhibition of galectin-1 function, as evident by the difference in sensitivity to LLS2 with galectin-1 protein suppression and ectopic expression.

LLS2 can potentiate the antitumor activity of paclitaxel on cancer cells

We examined the synergistic effects of LLS2 with some current chemotherapeutic drugs including docetaxel, paclitaxel, 5-fluorouracil (5-FU), oxaliplatin, carboplatin, doxorubicin, and gemcitabine *in vitro*. Our combination studies showed that LLS2 displays synergistic effects with docetaxel, paclitaxel, 5-FU, oxaliplatin, carboplatin, and doxorubicin. Among these chemotherapeutic drugs, paclitaxel is of particular interest, as it has a synergistic effect with LLS2 on many cancer cell lines. Paclitaxel (taxol), a very important chemotherapeutic agent, binds to microtubules to form highly stable microtubules, causing cell-cycle arrest at the G_2–M phase. In addition, paclitaxel also exerts apoptotic activity through the mitotic block (34). In clinical cancer therapy, paclitaxel is a potent and toxic antineoplastic drug commonly used to treat a wide variety of human malignancies, such as ovarian, breast, and non–small cell lung cancers. Single-agent and combination therapy have been extensively evaluated in clinical trials (35, 36). Because of its low solubility, paclitaxel is formulated in Cremophor, which requires premedication of patients with benadryl and dexamethasone. The drug has also been nanoformulated with human serum albumin (Abraxane). Compounds that can potentiate the antitumor effects of paclitaxel will be of great clinical interest.

In our study, we observed that paclitaxel exhibited moderate cytotoxicity against PC3 and SKOV3 cancer cells at 2 nmol/L. After the combined treatment with LLS2, much stronger antiproliferative effect was achieved (Fig. 5A). This synergistic effect was confirmed by measuring the CI (Fig. 5B), and it was further determined at various concentrations of LLS2 and paclitaxel against SKOV3 (Fig. 5c). Increased apoptosis and downregulation of pERK were also observed after combined LLS2/paclitaxel treatment for 24 hours (Fig. 5D and E).

LLS2 alone and LLS2/paclitaxel have antitumor activity *in vivo*

SKOV3 ovarian cancer xenograft model was used to examine the *in vivo* antitumor effect of LLS2. Both tumor size (Fig. 6A and B) and tumor weight (Fig. 6C) were smaller in LLS2-treated mice. Tumor response was found to be much more pronounced in the combination LLS2 and paclitaxel treatment group (Fig. 6A–C). Importantly, mice treated with the LLS2/paclitaxel combination regimen continued to gain weight and did not show any significant side effects (Fig. 6D). Excised tumors were analyzed for cleaved caspase-3 and Ki-67 level. Increased cleaved caspase-3–positive cells (~10-fold) and decreased Ki-67–positive cells were detected in LLS2-treated tumor, when compared with negative controls (Fig. 6E and F). Consistent with the *in vitro* and *in vivo* tumor response data, cleaved caspase-3–positive cells were dramatically increased, and Ki-67–positive cells were decreased in combination LLS2/paclitaxel–treated group as compared with the other three groups (Fig. 6E and F). Together, these results indicate that LLS2 is an excellent drug for the development of a novel therapeutic combination regimen with paclitaxel, for the

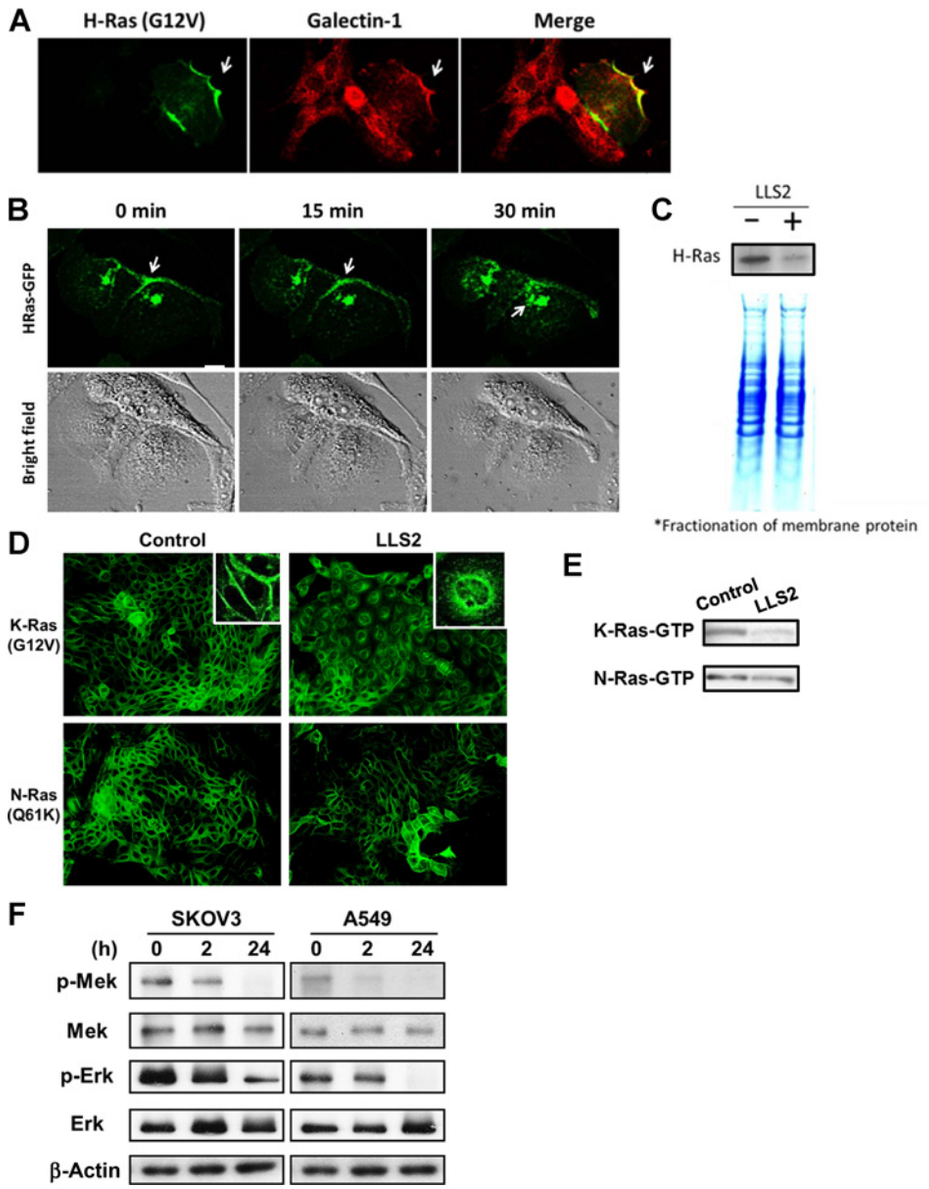

Figure 3.
LLS2 causes membrane dissociation of H- and K-Ras. **A,** Colocalization of galectin-1 and H-Ras. **B,** Once activated by EGF, H-Ras will be partially trafficked to the plasma membrane, leading to the activation of Erk pathway. After 15-minute treatment with LLS2 (25 μmol/L), there was a loss of membrane-localized H-Ras. Notably, intracellular H-Ras was augmented 30 minutes after LLS2 treatment. Scale bars, 25 μm. **C,** Quantification of membrane-associated H-Ras (active form) by immunoblot analysis after treatment with buffer (−) or LLS2 (+), showing that LLS2 was able to lower the level of activated H- and K-Ras. **D,** LLS2 also miscolocalized the EGF-stimulated K-Ras(G12V) but not N-Ras(Q61K). **E,** Quantification of activated K- and N-Ras. **F,** phospho-Mek and phospho-Erk were significantly downregulated after treatment with LLS2 (25 μmol/L) for 24 hours. Scale bars, 50 μm.

efficacious treatment of ovarian cancer and a number of other solid tumors.

Discussion

In this study, we have established the utility of benzimidazole-based OB2C combinatorial library, in conjunction with a high-throughput cell-based screening method to discover novel anticancer agents. Through screening a benzimidazole derivatives library (containing 74,088 discrete compounds), we have identified a novel proapoptotic compound LLS2. Further characterization of LLS2 revealed that galectin-1 is one of the target proteins and that LLS2 inhibits cell proliferation. Molecular modeling studies suggested that LLS2 binds to the interface between the dimeric galectin-1 subunits and is within 6 Å from the β-galactoside binding pocket. We have also demonstrated one molecular mechanism of action of LLS2 on cell death. Binding of LLS2 to galectin-1 decreases membrane-associated H-Ras and K-Ras and contributed to the suppression of pErk pathway. Moreover, we have found that LLS2 synergizes the anticancer effects of paclitaxel against several human cancer cell lines (ovarian cancer, pancreatic cancer, colon cancer, and breast cancer cells). In *in vivo* study, LLS2 significantly suppressed tumor growth and led to significant tumor regression when used in combination with paclitaxel in SKOV3 xenograft model. Our current study suggests that cell-based OB2C combinatorial screening method is feasible for drug discovery and that LLS2 compound could potentially be used as a lead compound to develop a novel anticancer drug.

Compared with normal tissues, galectin-1 is overexpressed in cancer tissues, and the level of galectin-1 in tumors has been reported to be positively correlated with clinical staging, suggesting that galectin-1 participates in tumor progression. Moreover, a

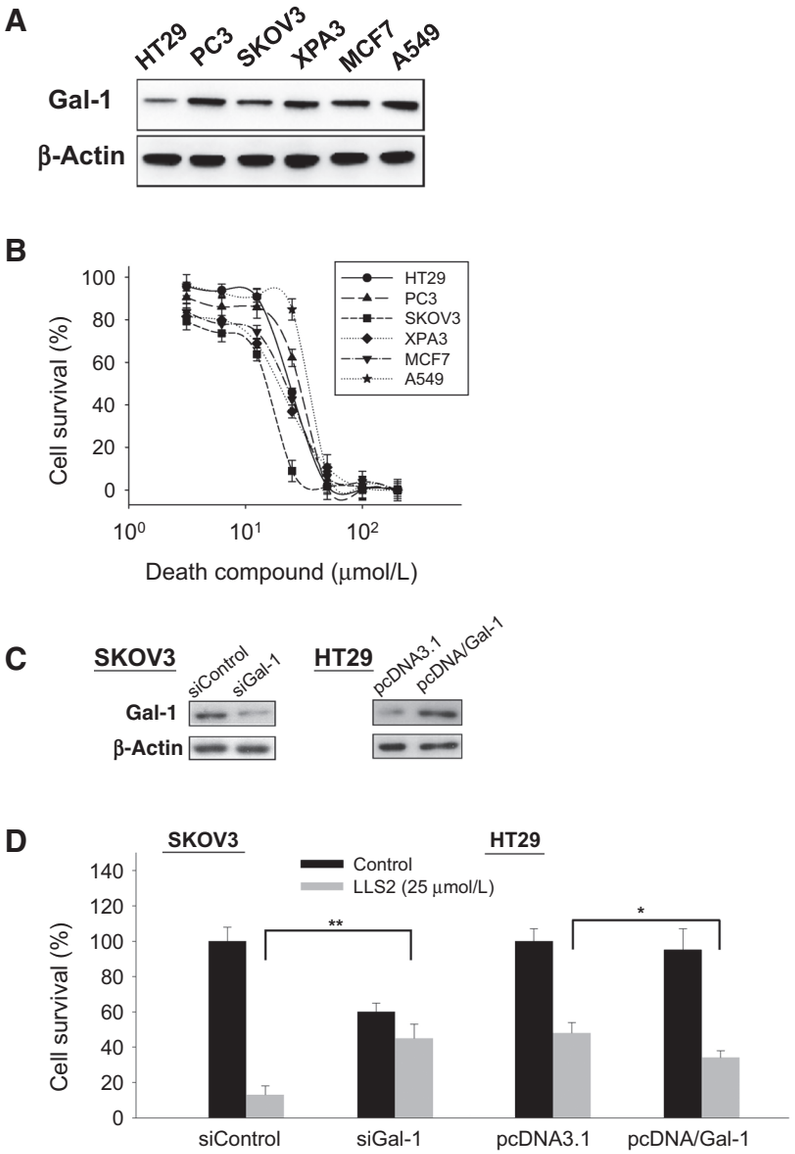

Figure 4.

In vitro anticancer activity of LL2. **A,** Endogenous expression of galectin-1 in six different cancer cells. **B,** Death ligand LLS2 (soluble form) kills a number of different cancer cell lines in solution. **C,** Immunoblots demonstrate the suppression of endogenous galectin-1 expression by siRNA in SKOV3 cells, and ectopic overexpression of galectin-1 in HT-29 cells. **D,** SKOV3 cells transfected with control siRNA, galectin-1 siRNA, and HT29 cells transfected with control pcDNA3.1; pcDNA/Gal-1 were treated with/without LLS2 (25 μmol/L) for 72 hours. *, $P < 0.05$; **, $P < 0.01$; ***, $P < 0.001$.

high level of galectin-1 expression has been found to correlate with poor prognosis in prostate, lung and ovarian cancers (15, 37, 38). Recent articles also reported that galectin-1 exerts an oncogenic activity through the activation of H-Ras/Raf/ERK pathway, p21, and Bcl-2 in ovarian cancer (14), HIF/mTOR pathway in clear cell renal cell carcinoma (18), and Hedgehog pathway in pancreatic cancer (19). Galectin-1 secreted by tumor cells could suppresses tumor immune response through the induction of apoptosis of activated T cells (23, 24). Taken together, in addition to exerting direct inhibitory effect on ERK pathway, LLS2 might also suppresses other galectin-1–related pathway. In our preliminary results, LLS2 inhibited galectin-1–related angiogenesis. Work is currently under way in our laboratory on examining those galectin-1–related mechanisms.

It has been suggested that the hydrophobic pocket of galectin-1 interacts with the farnesyl group of H-Ras, stabilizing H-Ras–GTP interaction with the cell membrane (39). A single point mutation (L11A) in the galectin-1 hydrophobic pocket displaces H-RasG12V from the plasma membrane and inhibits biological activity of Ras (39). As galectin-1's hydrophobic pocket is essential for the binding to H-Ras, we hypothesize that LLS2/galectin-1 interaction may change the property or conformation of the hydrophobic pocket in galectin-1 and therefore attenuate the binding of galectin-1 to membrane-associated H-Ras. This hypothesis, as well as how LLS2/galectin-1 interaction affects downstream targets, will need to be further confirmed.

Paz and colleagues (22) reported that membrane-associated galectin-1 binds oncogenic H-Ras to mediate Ras membrane anchorage, resulting in cell transformation. To date, only this study has addressed the membrane function of galectin-1; however, the larger role of membrane-associated galectin-1 in cancer is largely unknown. Our OB2C screening result demonstrates a new function of membrane galectin-1 as a death receptor, given that its interaction with LLS2 (as a proxy death ligand) leads to cell death.

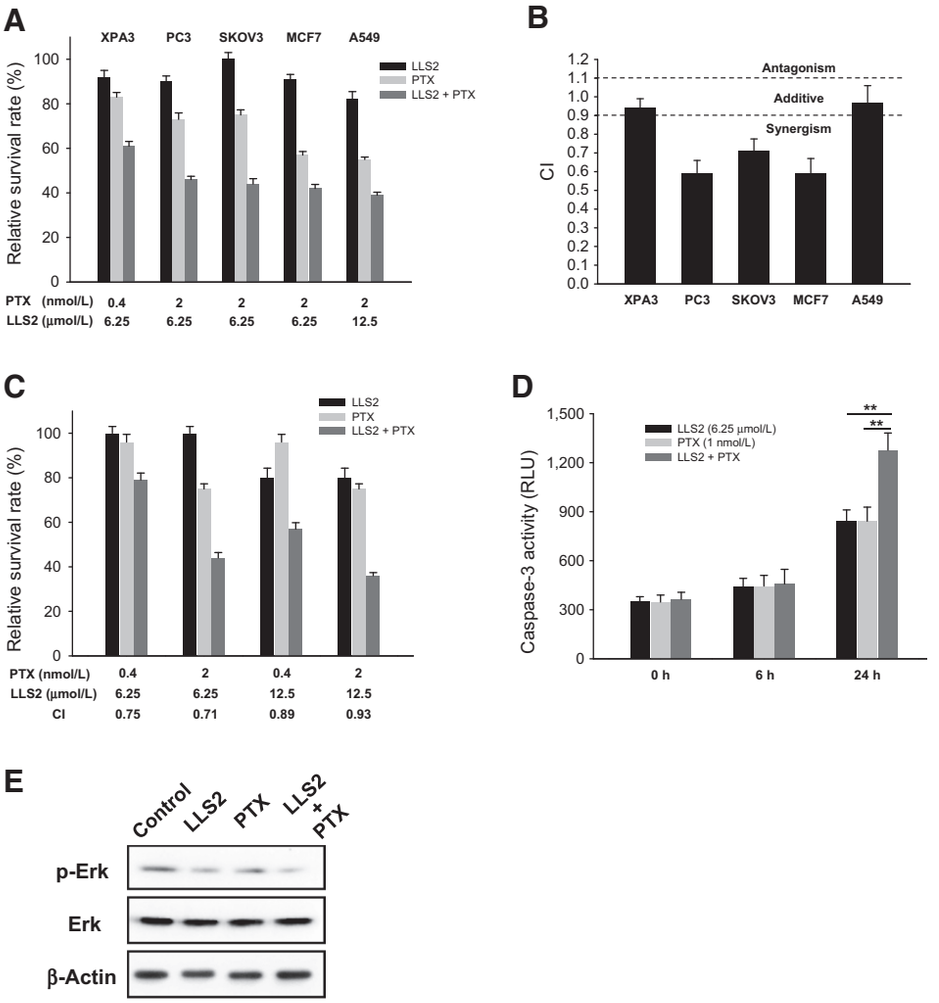

Figure 5.

LLS2 can potentiate the anticancer effects of paclitaxel (PTX). **A,** The cytotoxicity of LLS2 alone, PTX alone, and the combination of LLS2 and PTX. **B,** The CI of the treatment of combination of LLS2 and PTX. CI <0.9 indicates synergism, CI = 0.9–1.10 indicates additive interaction, and CI >1.1 indicates antagonism. **C,** LLS2 can potentiate the anticancer effects of PTX at various concentrations. **D** and **E,** Apoptosis was increased (**D**), and phospho-ERK was downregulated after combination treatment (**E**; LLS, 25 μmol/L and PTX, 1 nmol/L) in SKOV3 cells for 24 hours.

Therefore, not only has our OB2C screening discovered a novel LLS2 death ligand, but it has also opened a window for the future study of a new membrane function featuring galectin-1's role as a death receptor.

In contrast to biologicals, small molecules are orally bioavailable and their manufacturing cost is generally lower, which is an important advantage for patients and the health care system. Within the small-molecule compounds, the benzimidazole scaffold is a common therapeutic pharmacophore found in several bioactive compounds (7). Its pharmacologic activities include antiviral (40), antimicrobial (41, 42), antiparasitic (43), anti-inflammatory (44), and antihypertensive (45). Therefore, we chose the benzimidazole as the pharmacophore scaffold and utilized combinatorial chemistry to generate benzimidazole-based compounds.

MS analysis results of proteins pulled down by LLS2 also revealed nucleophosmin, heterogenous nuclear ribonucleoprotein, and filaggrin-2, making them potential therapeutic target proteins for LLS2. In fact, many FDA- approved and clinical effective drugs have been shown to act on multiple target proteins rather than a single target; examples are imatinib (Novartis) and sorafenib (Bayer). The main concern of off-target effects is toxicity. Thus far, no obvious toxicities have been observed in the LLS2-treated mice (Fig 6D). This and other published work strongly suggest that galectin-1 is an excellent therapeutic target against tumor; we therefore would like to further improve the binding specificity and affinity of LLS2 to galectin-1. The "R_2" group in LLS2 forms hydrogen bond with the galectin-1 dimer (Fig 2H); we could modify "R_1" and the central scaffold to provide additional hydrogen bonding contacts (e.g., K127) with the dimer interface. Moreover, the binding pocket for LLS2 is also close enough (within 6 Å) to the known sugar-binding pocket of galectin-1. This warrants the extension of our LLS2 virtual compound library to include sugar moieties attached by linkers of varying lengths to generate compounds that aim to target both the LLS2 and sugar-binding pockets. This approach not only allows us to improve the binding affinity and specificity of the compound to galectin-1, but also inhibit the functional effect of glycan binding to galectin-1.

Considering the multitude of molecular entities and signaling pathways regulating the proliferation and cellular survival/cell death, the inhibition of a single target gene or transcriptional factor may not be sufficient to suppress neoplastic progression. In clinical oncology, cancer drugs with different mechanism of actions are often given in combination to maximize the therapeutic effects, decrease side effects, and delay drug resistance (46). In this study, we have clearly demonstrated that LLS2 could

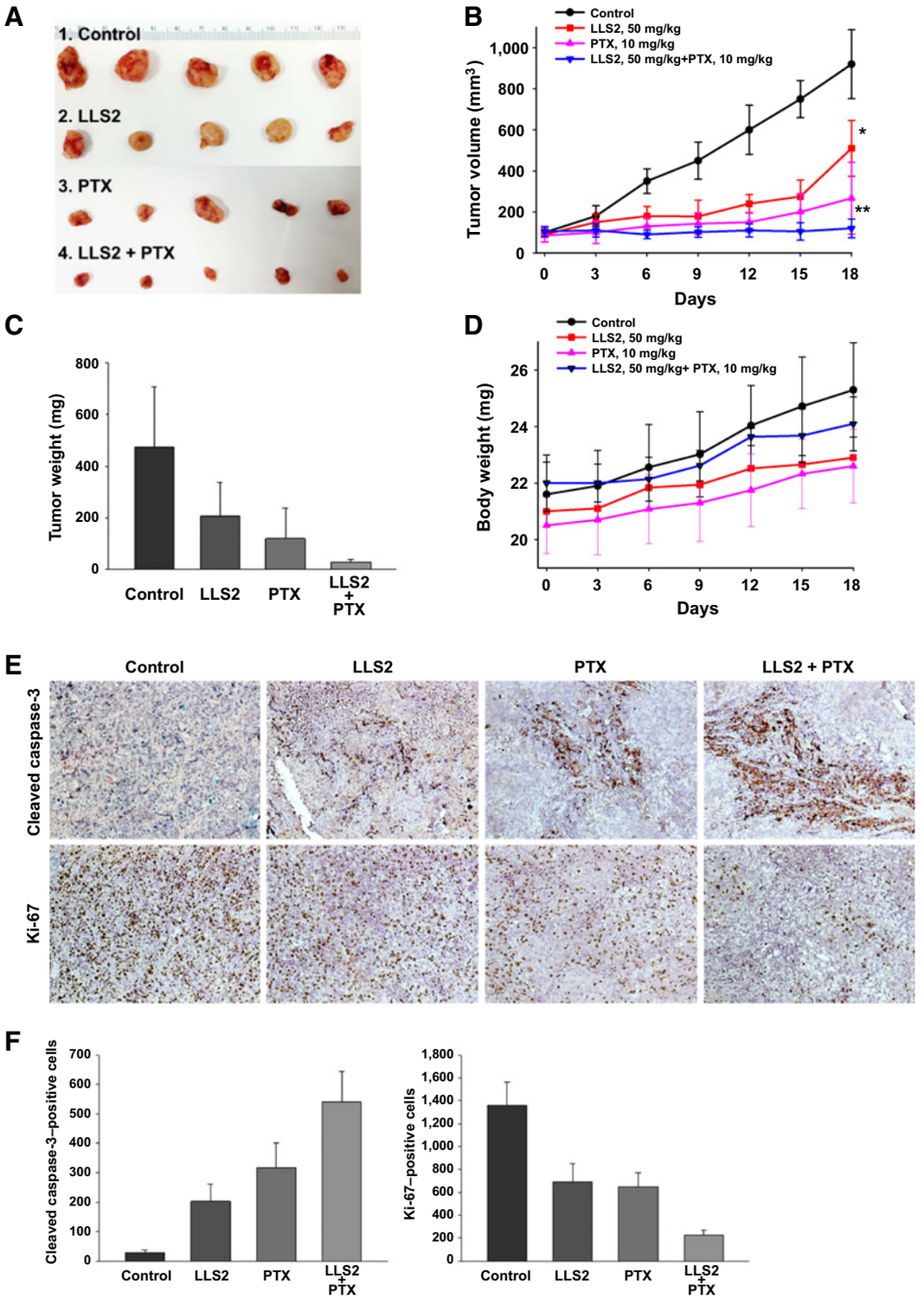

Figure 6.

LLS2 alone and LLS2/PTX have antitumor activity in SKOV3 xenograft model. **A,** Xenograft tumor. **B** and **C,** Tumor growth curves (**B**) and tumor weight of the xenografts in inoculated nude mice (**C**). **D,** Body weight of nude mice. Briefly, 2.5×10^6 SKOV3 cells were subcutaneously injected to the right side of the dorsal flank of the female congenital athymic BALB/c nude mice. The tumors were allowed to grow to about 100 mm^3. Then, mice were randomly divided into control and treatment groups ($n = 5$). Mice were given a daily intravenous administration for 5 successive days. **E,** IHC detection of Ki-67 and cleaved caspase-3 expression. **F,** Quantification of immunostaining of Ki-67 and cleaved caspase-3–positive cells. The cells were counted in 3 random chosen areas. *, $P < 0.05$; **, $P < 0.01$.

synergize the antitumor efficacy of paclitaxel, both *in vitro* (Fig. 5) and *in vivo* (Fig. 6). We will further explore this synergy in xenograft model, patient-derived xenograft model and canine spontaneous tumor model. Understanding the mechanism of this synergy may allow us to develop more efficacious drug combinations against human cancer.

In conclusion, through screening OB2C combinatorial small-molecule libraries, we have identified LLS2 as the "death ligand." Galectin-1 is the target of LLS2, and binding of LLS2 to galectin-1 decreases membrane-associated H-Ras and K-Ras and contributes to the suppression of MAPK/ERK pathway. LLS2 exerts antitumor activity, and it can also potentiate the anticancer effects of paclitaxel in SKOV3 xenograft model. LLS2 is a promising lead compound to be developed into a potent antitumor drug, and LLS2/paclitaxel combination treatment is a potential new approach to enhance the therapeutic effects of paclitaxel, a very important cytotoxic chemotherapeutic drug clinically active against many different cancer types.

Disclosure of Potential Conflicts of Interest

No potential conflicts of interest were disclosed.

Authors' Contributions

Conception and design: T.-C. Shih, R. Liu, K.S. Lam
Development of methodology: T.-C. Shih, R. Liu, G. Fung, G. Bhardwaj
Acquisition of data (provided animals, acquired and managed patients, provided facilities, etc.): T.-C. Shih, R. Liu, G. Fung
Analysis and interpretation of data (e.g., statistical analysis, biostatistics, computational analysis): T.-C. Shih, R. Liu, G. Fung, G. Bhardwaj, P.M. Ghosh, K.S. Lam
Writing, review, and/or revision of the manuscript: T.-C. Shih, R. Liu, P.M. Ghosh, K.S. Lam
Administrative, technical, or material support (i.e., reporting or organizing data, constructing databases): T.-C. Shih
Study supervision: T.-C. Shih, K.S. Lam

Acknowledgments

We thank Drs. A.W. Herren and B.S. Phinney (UC Davis Genome Center, University of California Davis, Davis) for performing LC/MS-MS. The authors would like to thank the Combinatorial Chemistry Shared Resource at the University of California Davis for assistance with synthesis and screening of OB2C libraries.

Grant Support

This work was supported by grants from the NIH/NCI (2R33 CA160132; to K. S. Lam). Utilization of the Combinatorial Chemistry Shared Resource was supported by the UC Davis Comprehensive Cancer Center support grant (NCI P30CA093373).

The costs of publication of this article were defrayed in part by the payment of page charges. This article must therefore be hereby marked *advertisement* in accordance with 18 U.S.C. Section 1734 solely to indicate this fact.

Received October 18, 2016; revised December 16, 2016; accepted April 3, 2017; published OnlineFirst April 10, 2017.

References

1. Engel A, Gaub HE. Structure and mechanics of membrane proteins. Annu Rev Biochem 2008;77:127–48.
2. Akira S, Takeda K. Toll-like receptor signalling. Nat Rev Immunol 2004;4:499–511.
3. Ritter SL, Hall RA. Fine-tuning of GPCR activity by receptor-interacting proteins. Nat Rev Mol Cell Biol 2009;10:819–30.
4. Croft M, Benedict CA, Ware CF. Clinical targeting of the TNF and TNFR superfamilies. Nat Rev Drug Discov 2013;12:147–68.
5. Sharma SV, Bell DW, Settleman J, Haber DA. Epidermal growth factor receptor mutations in lung cancer. Nat Rev Cancer 2007;7:169–81.
6. Piechocki MP, Wu GS, Jones RF, Jacob JB, Gibson H, Ethier SP, et al. Induction of proapoptotic antibodies to triple-negative breast cancer by vaccination with TRAIL death receptor DR5 DNA. Int J Cancer 2012; 131:2562–72.
7. Sivakumar R, Pradeepchandran R, Jayaveera KN, Kumarnallasivan P, Vijaianand PR, Venkatnarayanan R. Benzimidazole: an attractive pharmacophore in medicinal chemistry. IJPR 2011;3:19–31.
8. Lam KS, Salmon SE, Hersh EM, Hruby VJ, Kazmierski WM, Knapp RJ. A new type of synthetic peptide library for identifying ligand-binding activity. Nature 1991;354:82–4.
9. Sweeney MC, Pei D. An improved method for rapid sequencing of support-bound peptides by partial edman degradation and mass spectrometry. J Comb Chem 2003;5:218–22.
10. Marani MM, Oliveira E, Cote S, Camperi SA, Albericio F, Cascone O. Identification of protein-binding peptides by direct matrix-assisted laser desorption ionization time-of-flight mass spectrometry analysis of peptide beads selected from the screening of one bead-one peptide combinatorial libraries. Anal Biochem 2007;370:215–22.
11. Peng L, Liu R, Marik J, Wang X, Takada Y, Lam KS. Combinatorial chemistry identifies high-affinity peptidomimetics against alpha4beta1 integrin for in vivo tumor imaging. Nat Chem Biol 2006;2:381–9.
12. Meldal M. The one-bead two-compound assay for solid phase screening of combinatorial libraries. Biopolymers 2002;66:93–100.
13. Kumaresan PR, Wang Y, Saunders M, Maeda Y, Liu R, Wang X, et al. Rapid discovery of death ligands with one-bead-two-compound combinatorial library methods. ACS Comb Sci 2011;13: 259–64.
14. Zhang P, Zhang P, Shi B, Zhou M, Jiang H, Zhang H, et al. Galectin-1 overexpression promotes progression and chemoresistance to cisplatin in epithelial ovarian cancer. Cell Death Dis 2014;5:e991.
15. van den Brûle FA, Waltregny D, Castronovo V. Increased expression of galectin-1 in carcinoma-associated stroma predicts poor outcome in prostate carcinoma patients. J Pathol 2001;193:80–7.
16. Carlini MJ, Roitman P, Nunez M, Pallotta MG, Boggio G, Smith D, et al. Clinical relevance of galectin-1 expression in non-small cell lung cancer patients. Lung Cancer 2014;84:73–8.
17. Jung EJ, Moon HG, Cho BI, Jeong CY, Joo YT, Lee YJ, et al. Galectin-1 expression in cancer-associated stromal cells correlates tumor invasiveness and tumor progression in breast cancer. Int J Cancer 2007;120:2331–8.
18. White NM, Masui O, Newsted D, Scorilas A, Romaschin AD, Bjarnason GA, et al. Galectin-1 has potential prognostic significance and is implicated in clear cell renal cell carcinoma progression through the HIF/mTOR signaling axis. Br J Cancer 2014;110:1250–9.
19. Martinez-Bosch N, Fernandez-Barrena MG, Moreno M, Ortiz-Zapater E, Munne-Collado J, Iglesias M, et al. Galectin-1 drives pancreatic carcinogenesis through stroma remodeling and hedgehog signaling activation. Cancer Res 2014;74:3512–24.
20. Demydenko D, Berest I. Expression of galectin-1 in malignant tumors. Exp Oncol 2009;31:74–9.
21. Liu FT, Rabinovich GA. Galectins as modulators of tumour progression. Nat Rev Cancer 2005;5:29–41.
22. Paz A, Haklai R, Elad-Sfadia G, Ballan E, Kloog Y. Galectin-1 binds oncogenic H-Ras to mediate Ras membrane anchorage and cell transformation. Oncogene 2001;20:7486–93.
23. Perillo NL, Pace KE, Seilhamer JJ, Baum LG. Apoptosis of T cells mediated by galectin-1. Nature 1995;378:736–9.
24. Rubinstein N, Alvarez M, Zwirner NW, Toscano MA, Ilarregui JM, Bravo A, et al. Targeted inhibition of galectin-1 gene expression in tumor cells results in heightened T cell-mediated rejection. Cancer Cell 2004;5:241–51.
25. Stanley P. Galectin-1 pulls the strings on VEGFR2. Cell 2014;156:625–6.
26. Xiao W, Li T, Bononi FC, Lac D, Kekessie IA, Liu Y, et al. Discovery and characterization of a high-affinity and high-specificity peptide ligand LXY30 for *in vivo* targeting of alpha3 integrin-expressing human tumors. EJNMMI Res 2016;6:18.

27. Chou TC, Talalay P. Generalized equations for the analysis of inhibitions of michaelis-menten and higher-order kinetic systems with two or more mutually exclusive and nonexclusive inhibitors. Eur J Biochem 1981;115: 207–16.
28. Hsieh SY, Shih TC, Yeh CY, Lin CJ, Chou YY, Lee YS. Comparative proteomic studies on the pathogenesis of human ulcerative colitis. Proteomics 2006;6:5322–31.
29. Xiao K, Li Y, Lee JS, Gonik AM, Dong T, Fung G, et al. "OA02" peptide facilitates the precise targeting of paclitaxel-loaded micellar nanoparticles to ovarian cancer *in vivo*. Cancer Res 2012;72:2100–10.
30. Nicholson DW, Thornberry NA. Caspases: killer proteases. Trends Biochem Sci 1997;22:299–306.
31. Hug H, Los M, Hirt W, Debatin K-M. Rhodamine 110-linked amino acids and peptides as substrates to measure caspase activity upon apoptosis induction in intact cells. Biochemistry 1999;38:13906–11.
32. Julie E, Thuy N, Douglas C, Dafna L, Reuben L. Differential expression of endogenous galectin-1 and galectin-3 in human prostate cancer cell lines and effects of overexpressing galectin-1 on cell phenotype. Int J Oncol 1999;14:217–24.
33. Anjum R, Blenis J. The RSK family of kinases: emerging roles in cellular signalling. Nat Rev Mol Cell Biol 2008;9:747–58.
34. Jordan MA, Wendell K, Gardiner S, Brent Derry W, Copp H, Wilson L. Mitotic block induced in hela cells by low concentrations of paclitaxel (taxol) results in abnormal mitotic exit and apoptotic cell death. Cancer Res 1996;56:816–25.
35. Piccart MJ, Bertelsen K, James K, Cassidy J, Mangioni C, Simonsen E, et al. Randomized intergroup trial of cisplatin–paclitaxel versus cisplatin–cyclophosphamide in women with advanced epithelial ovarian cancer: three-year results. J Natl Cancer Inst 2000;92:699–708.
36. Malingré MM, Terwogt JMM, Beijnen JH, Rosing H, Koopman FJ, Tellingen Ov, et al. Phase I and pharmacokinetic study of oral paclitaxel. J Clin Oncol 2000;18:2468–75.
37. Kim HJ, Jeon HK, Cho YJ, Park YA, Choi JJ, Do IG, et al. High galectin-1 expression correlates with poor prognosis and is involved in epithelial ovarian cancer proliferation and invasion. Eur J Cancer 2012;48:1914–21.
38. Szoke T, Kayser K, Baumhakel JD, Trojan I, Furak J, Tiszlavicz L, et al. Prognostic significance of endogenous adhesion/growth-regulatory lectins in lung cancer. Oncology 2005;69:167–74.
39. Rotblat B, Niv H, André S, Kaltner H, Gabius HJ, Kloog Y. Galectin-1(L11A) predicted from a computed galectin-1 farnesyl-binding pocket selectively inhibits ras-GTP. Cancer Res 2004;64:3112–8.
40. Tewari AK, Mishra A. Synthesis and antiviral activities of N-substituted-2-substituted-benzimidazole derivatives. Indian J Chem 2006;45B: 489–93.
41. Mavrova A, Anichina KK, Vuchev DI, Tsenov JA, Kondeva MS, Micheva MK. Synthesis and antitrichinellosis activity of some 2-substituted-[1,3]thiazolo[3,2-a]benzimidazol-3(2H)-ones. Biorg Med Chem 2005; 13:5550–9.
42. Örena İ, Temiza Ö, Yalçna İ, Şenera E, Altanlarb N. Synthesis and antimicrobial activity of some novel 2,5- and/or 6-substituted benzoxazole and benzimidazole derivatives. Eur J Pharm Sci 1998;7:153–60.
43. Valdez J, Cedillo R, Hernández-Campos A, Yépez L, Hernández-Luis F, Navarrete-Vázquez G, et al. Synthesis and antiparasitic activity of 1H-benzimidazole derivatives. Bioorg Med Chem Lett 2002;12:2221–4.
44. Sondhi SM, Rajvanshi S, Johar M, Bharti N, Azam A, Singh AK. Anti-inflammatory, analgesic and antiamoebic activity evaluation of pyrimido[1,6-a]benzimidazole derivatives synthesized by the reaction of ketoisothiocyanates with mono and diamines. Eur J Med Chem 2002;37:835–43.
45. Kumar JR, Jawahar LJ, Pathak DP. Synthesis of benzimidazole derivatives: as anti-hypertensive agents. E J Chem 2006;3:278–85.
46. Jemal A, Murray T, Ward E, Samuels A, Tiwari RC, Ghafoor A, et al. Cancer statistics, 2005. CA Cancer J Clin 2005;55:10–30.